THE ASTROPHYSICAL JOURNAL, 449:105–118, 1995 August 10

OSSE OBSERVATIONS OF GAMMA-RAY EMISSION FROM CENTAURUS A

R. L. KINZER, W. N. JOHNSON, C. D. DERMER, J. D. KURFESS, M. S. STRICKMAN, J. E. GROVE, AND R. A. KROEGER
E. O. Hulburt Center for Space Research, Naval Research Laboratory, Washington, DC 20375-5320
D. A. GRABELSKY, W. R. PURCELL, AND M. P. ULMER
Department of Physics and Astronomy, Northwestern University, Evanston, IL 60208
G. V. JUNG
Universities Space Research Association, Washington, DC 20024
AND
K. MCNARON-BROWN
George Mason University, Fairfax, VA 22030
Received 1994 November 22; accepted 1995 February 23

ABSTRACT

Results are reported on hard X-ray and soft gamma-ray observations of Centaurus A during 1991–1994 with the Oriented Scintillation Spectrometer Experiment (OSSE) on NASA's *Compton Gamma Ray Observatory* (*CGRO*). Long-term intensity changes by a factor of 2–3 were measured over this period. Short-term variations by as much as 25% on timescales as short as 12 hr were detected in most of the observations. No evidence for gamma-ray line emission was detected at sensitivities much improved over previous observations. An intensity-dependent evolution of the 50–1000 keV spectral shape was observed which can be characterized as an exponentially cut-off power law with an intensity-dependent cutoff energy ranging from ~ 300 keV at the highest observed level to ~ 700 keV at the lowest levels. A broken power-law model with an intensity-correlated break above ~ 120 keV describes the observed spectral changes equally well. Best-fit spectral breaks vary from $\Delta\Gamma \sim 0.25 \pm 0.1$ at the lowest levels to $\Delta\Gamma \sim 0.7 \pm 0.15$ at the highest observed intensity. Below 120 keV the spectra at all intensities can be fitted with photon spectral index $\Gamma \sim 1.70 \pm 0.08$, in agreement with prevous X-ray measurements. Contemporaneous measurements by the EGRET instrument on *CGRO* require additional spectral softening in the MeV region relative to broken power-law extrapolations of the OSSE measurements. At the maximum observed intensity, the luminosity of Cen A appears to peak at ~ 200 keV with $L_\gamma(50\text{–}1000 \text{ keV}) \approx 7 \times 10^{42}$ ergs s^{-1}, implying a minimum black hole mass of only $\approx 5 \times 10^4$ solar masses for Eddington-limited accretion.

Subject headings: galaxies: individual (NGC 5128) — gamma rays: observations — X-rays: galaxies

1. INTRODUCTION

The radio galaxy Centaurus A (NGC 5128) at ~ 5 Mpc ($z \cong 0.0008$; a Hubble constant $H_0 = 50$ km s^{-1} Mpc^{-1} is used throughout this work) is among the brightest objects in the sky at 100 keV and is one of the nearest galaxies with an active nucleus. Prior to the launch of the *Compton Gamma Ray Observatory* (*CGRO*), Cen A was one of four active galactic nuclei (AGNs) detected above 100 keV (see, e.g., Bassani & Dean 1983 for a summary) and was the brightest AGN at these energies. This peculiar elliptical galaxy has extended outer, middle, and inner radio lobes and an X-ray, optical, infrared, and radio jet aligned with the inner lobes. An active compact core observed at X-ray (Feigelson et al. 1981), infrared (Giles 1986; Joy et al. 1991), submillimeter (Hawarden et al. 1993), and radio (Burns, Feigelson, & Schreier 1983; Preston et al. 1983; Meier et al. 1989) frequencies is thought to power the jet and lobe structure (see Ebneter & Balick 1983 for a review of early work). Although not exceptionally luminous for an AGN ($\lesssim 10^{43}$ ergs s^{-1}), it has a high apparent brightness and thus provides an excellent opportunity to measure the high-energy characteristics of an AGN. Over the past two decades Cen A has been observed to vary by an order of magnitude at X-ray energies (e.g., Jourdain et al. 1993 and references therein). Prior to the *CGRO* observations discussed here, a number of gamma-ray observations of Cen A were performed to extend measurements to energies above 100 keV (e.g., Grindlay et al. 1975; Hall et al. 1976; Baity et al. 1981; Pietsch et al. 1981; Gehrels et al. 1984; von Ballmoos et al. 1987; O'Neill et al. 1989; Bignami et al. 1979; Pollock et al. 1981). Emission was detected in the soft gamma-ray range, but only upper limits were obtained in the 100 MeV region.

The relatively weak radio luminosity ($\sim 10^{40}$ ergs s^{-1}) and the twin jet radio structure of Cen A place it in the category of FR I radio galaxies. Optical observations of fluorescent [O III] emission (Morganti et al. 1991, 1992) demonstrate the presence of intense beamed optical emission directed away from our viewing direction, in accord with the interpretation that Cen A is a misaligned blazar (Bailey et al. 1986). Understanding this source will provide important clues to the spectral behavior of radio-loud AGNs, which is also important in understanding the origin of the observed extragalactic gamma-ray background.

In this paper, we report results of the most sensitive hard X-ray and soft gamma-ray observations of Cen A to date. Measurements between 40 keV and 10 MeV by the Oriented Scintillation Spectrometer Experiment (OSSE) on NASA's *CGRO* were obtained from five observations of 2 weeks or shorter distributed over a 28 month period between 1991 October and 1994 February. A preliminary report covering a portion of this data was given by Kinzer et al. (1994). The

measurement procedures are described in § 2. Observed temporal variability and spectral measurements are presented in § 3. Results and comparisons with previous work are discussed in § 4, where we also discuss implications of the observations on the emission mechanism of the source. Conclusions are presented in § 5.

2. OBSERVATIONS AND DATA ANALYSIS

The OSSE instrument comprises four identical and independent phoswich spectrometers with a total area of 2620 cm^2 and an effective area of $\sim$2000 cm^2 at 511 keV (see Johnson et al. 1993 for an instrument description). The detectors are sensitive to gamma rays between about 0.04 and 10 MeV and have a resolution of $\sim$8.8% at 0.511 MeV. Each detector has an aperture of $\sim$3°.8 by 11°.4 full width at half-maximum (FWHM) defined by a passive tungsten slat collimator and is independently orientable in the narrow-angle direction. Cen A observations were conducted and processed in the manner described by Johnson et al. (1993).

Table 1 gives several relevant details of the five Cen A measurements made in 1991–1994. In each observation program or viewing period (VP), all four detectors were operated in a source/background chopping mode in which each detector alternately viewed the source for 2 minutes and one of two background fields for 2 minutes. Variations in the collimator orientation, the background offset angles, and the source pointing directions among the four observations were used to assess contamination of the Cen A measurements by nearby weak sources in either the source or background fields.

When considering contamination by nearby sources, it should be remembered that Cen A is the brightest extragalactic X-ray source, and among the brightest of all X-ray sources; none of the nearby X-ray sources has an X-ray intensity greater than 10% of the lowest observed intensity of Cen A at the same energy. Standard Cen A source observations with alternating symmetrical 4°.5 background-field offset angles were made in the 1991 (VP 12) and 1992 (VP 43) measurements at position angles differing by $\sim$73° (Table 1), providing only partially common source and background fields in the two observations. Comparison of these two observations provides limits on contributions of potentially confusing nearby sources.

Preliminary analyses of EGRET observations provided weak detections of two sources, GRO J1317−44 (Hartman 1992) and GRO J1329−43 (Hartman 1994), near Cen A at energies above 100 MeV. These sources at 1°.8 and 1°.1, respectively, from Cen A were judged by the EGRET team to be inconsistent with the position of Cen A. Possible contributions from GRO J1317−44 were assessed during the 1993 (VP 215/217) OSSE observation by alternately observing its position and that of Cen A. An upper limit to contributions from this source of 10% of the measured Cen A flux was determined in these interleaved observations. No improvements in the fits were achieved by including this source in the modeling. Although GRO J1329−43 was not reported by EGRET prior to this observation, its position (as determined by EGRET in 1994) was favorably aligned such that an upper limit to its contributions of $\sim$20% of the measured Cen A flux was also set during the VP 215/217 observation. Recent reprocessing of these EGRET data using an improved background model indicates the presence of a 5 σ source which is compatible with the position of Cen A. Emission from up to three sources still cannot be ruled out by the data, however (Hartman 1995).

The potentially most serious confusion at high energies is from the X-ray–selected (0.3–3.5 keV) BL Lac candidate 1E 1312−4221 (Stocke et al. 1990), which is $\sim$2°.0 from Cen A with a 1 keV intensity of 1%–10% of the historically observed range of Cen A intensities (e.g., Feigelson et al. 1981). It has an X-ray–to–optical spectral index of 0.84. Although it has not been detected at higher X-ray energies, marginal EGRET detection of this source above 100 MeV in one viewing period was reported by Fichtel et al. (1994) (no spectral shape was reported). If a single power law from soft X-ray to gamma-ray energies represents this spectrum, then no significant contamination from this source is expected for OSSE observations. However, based on the possible broken power-law nature of the spectrum of the two BL Lac objects so far detected at soft gamma-ray energies (PKS 2155−304 and H1517+656), and the broken power-law nature of most other blazar spectra (McNaron-Brown et al. 1995), significant contributions above the OSSE sensitivity range cannot be ruled out. During VP 12 and VP 215/217 this source was at 75% response in the OSSE collimator. Because of different position angles (Table 1) and background field configurations, it was at 28% response in VP 43 and at 45% response in VP 316. These three configurations provide a means to assess any confusion introduced by this source.

Comparisons of the four Cen A observations at energies below 120 keV in the light of these observational differences show no spectral features which might suggest background or source field contamination in the observations. At higher energies, there are no indications of source confusion, but it will require specially designed observations to be certain that there is no contribution at higher energies from 1E 1312−4221. Despite the above reservations, in the current analysis we will assume that all measured flux above background originated in Cen A.

TABLE 1

OSSE CENTAURUS A OBSERVATIONS

Dates	Viewing Period	Live Time[a]	Collimator Orientation[b]	Simultaneous EGRET/COMPTEL Observations
1991 October 17–31	12	5.6	68°	Yes
1992 October 29–November 3	43	1.3	151	No
1993 April 1–6	215	1.1	60	Yes
1993 April 12–20	217	1.7	60	Yes
1994 February 23–March 2	316	4.4	145	Yes

[a] Total livetimes for background-subtracted and screened data in units of 10^5 s per single-detector equivalent effective area on source.

[b] Galactic position angle (angle relative to Galactic north) of the long direction of the collimator.

3. EXPERIMENTAL RESULTS

3.1. *Source Intensity*

OSSE observed Cen A in five sessions of duration between 5 and 14 days in the period 1991 October through 1994 February. The 1992, 1993, and 1994 emission levels were at or near the lowest intensities yet reported in the 50–100 keV energy band (Maisack et al. 1992; Ubertini et al. 1993). Figure 1 shows the 40–500 keV integral intensity history of the five observations at 12 and 24 hr timescales (note that the time axes are discontinuous). Average intensity levels for each individual interval are indicated by the dotted lines. Because the 1991 observation appears to have two distinct levels, it has been treated in the analysis as two separate observations.

One striking feature in Figure 1 is the sudden decrease in mean intensity level of about 25% on day 297 of 1991. Variations of equivalent magnitude observed at other times are more consistent with short-term changes about a nominal level. We have investigated the timescales for which the OSSE can detect short-term increases and decreases. Table 2 gives the χ^2 probabilities that the observed 40–500 keV intensities, binned over a range of timescales, are consistent with a normal distribution about the local mean intensities. The most significant variability is at timescales of 12 to 36 hr. Evidence for significant changes at a 6 hr timescale remains in the 1991 high-level data and in the second 1993 interval. Only the (short) first interval of the 1993 observation is consistent with no detected variability at any timescale. As a check that the variations observed from Cen A are not from some systematic effect in the data analysis, a similar analysis was performed on OSSE observations of the Crab Nebula, a constant source. These data were consistent with a constant intensity.

The increasing probabilities of normal statistical behavior at timescales greater than 36 hr, together with the persistent intensity level change observed in the 1991 data, are consistent with a model in which the source undergoes short-term changes relative to an underlying quiescent intensity level lasting for roughly 1 week or more. As can be seen by examining Figure 1, the average magnitudes of the most significant short-term changes are similar between periods despite the factor of 2–3 difference in average intensities. To further test the short-term variation trend, the data from the six intervals (Fig. 1) were divided into two bands with roughly equivalent statistical weight (40–100 keV and 100–500 keV). Linear correlation analyses were performed on the simultaneous intensity variations relative to the local mean in these bands for the ensemble of measurements. Correlation probabilities that intensity changes in each band are from independent distributions (i.e., are not correlated) were determined at timescales from 12 to 48 hr. Resulting probabilities are: 0.002, 0.005, 0.005, and 0.05 at 12, 24, 36, and 48 hr timescales, respectively. This strong correlation of intensity changes in the two independent energy bands indicates a common source region for the full 40–500 keV radiation band. The change in intensity level which occurred in about 1 day between contiguous intervals on day 297 of 1991 (Fig. 1) is strongly energy correlated and thus supports this conclusion. This intensity change is consistent with an energy-independent timescale, although the data do not permit an accurate assessment of energy dependence of variations at the 1 day timescale.

3.2. *Spectral Analysis*

The variations observed with OSSE in Cen A's emission level provide an opportunity to study the spectral shape as a function of intensity. During these observations, Cen A was in the intermediate to low intensity range relative to previously observed intensities, with the 1992–1994 observations being at historically low levels near 50 keV. Because Cen A was at comparable low intensities during the 1992–1994 observations, we have combined these lower significance observations to obtain a single high-statistics spectrum for model comparisons. Fits to the separate observations in 1992, 1993, and 1994 are consistent with fits to this composite spectrum. Time-integrated spectra from the full 1991 observation and the composite 1992–1994 observations are shown in $E^2\Phi(E)$ plots in Figures 2*a* and 2*b*, respectively [E is the photon energy and $\Phi(E)$ is the photon flux density].

We have chosen to fit these data using four spectral forms that are representative of models commonly used to explain the emission from AGNs. These include a single power law, a broken power law, an exponentially cut-off power law, and a thermal bremsstrahlung spectrum (see Table 3 for model descriptions). The single power law spectrum characterizes simple nonthermal origins for the radiation. The exponentially cut-off power law can parameterize the shapes of models having a power law form at low energies but which roll off at high energies, such as thermal Comptonization in an optically thin medium (e.g., Zdziarski et al. 1994; Hua & Titarchuk 1995) and off-axis jet emission models at energies below the sharp high-energy cutoff (Skibo, Dermer, & Kinzer 1994). The broken power law is not a spectral shape with a strong physical basis, but it is treated for comparison with previous work and because it provides a simple characterization of the data. It can approximate a variety of nonthermal mechanisms such as inverse Compton scattering. The thermal bremsstrahlung model is representative of models invoking thermal emission from hot media. The differences in these four spectral forms are

TABLE 2

χ^2 PROBABILITIES[a] OF STEADY EMISSION

OBSERVATION INTERVAL	TIME INTERVAL					
	6 hr	12 hr	24 hr	36 hr	48 hr	60 hr
1991 (Higher intensity).....	2.1×10^{-4}	5.4×10^{-6}	4.6×10^{-6}	8.3×10^{-4}	0.49	0.048
1991 (Lower intensity)	0.049	2.7×10^{-3}	0.023	1.2×10^{-3}	0.32	1.2×10^{-3}
1992.....	0.025	0.093	0.021	0.075	2.1×10^{-3}	0.082
1993 (First interval)	0.20	0.21	0.37	0.46	0.36	0.064
1993 (Second interval)	2.6×10^{-3}	4.8×10^{-3}	3.3×10^{-4}	2.2×10^{-4}	1.0×10^{-3}	0.10
1994.....	0.015	1.5×10^{-4}	6.0×10^{-6}	4.5×10^{-6}	9.4×10^{-5}	1.9×10^{-5}

[a] Probability that a greater χ^2 value would be found for intensities normally distributed about the local mean.

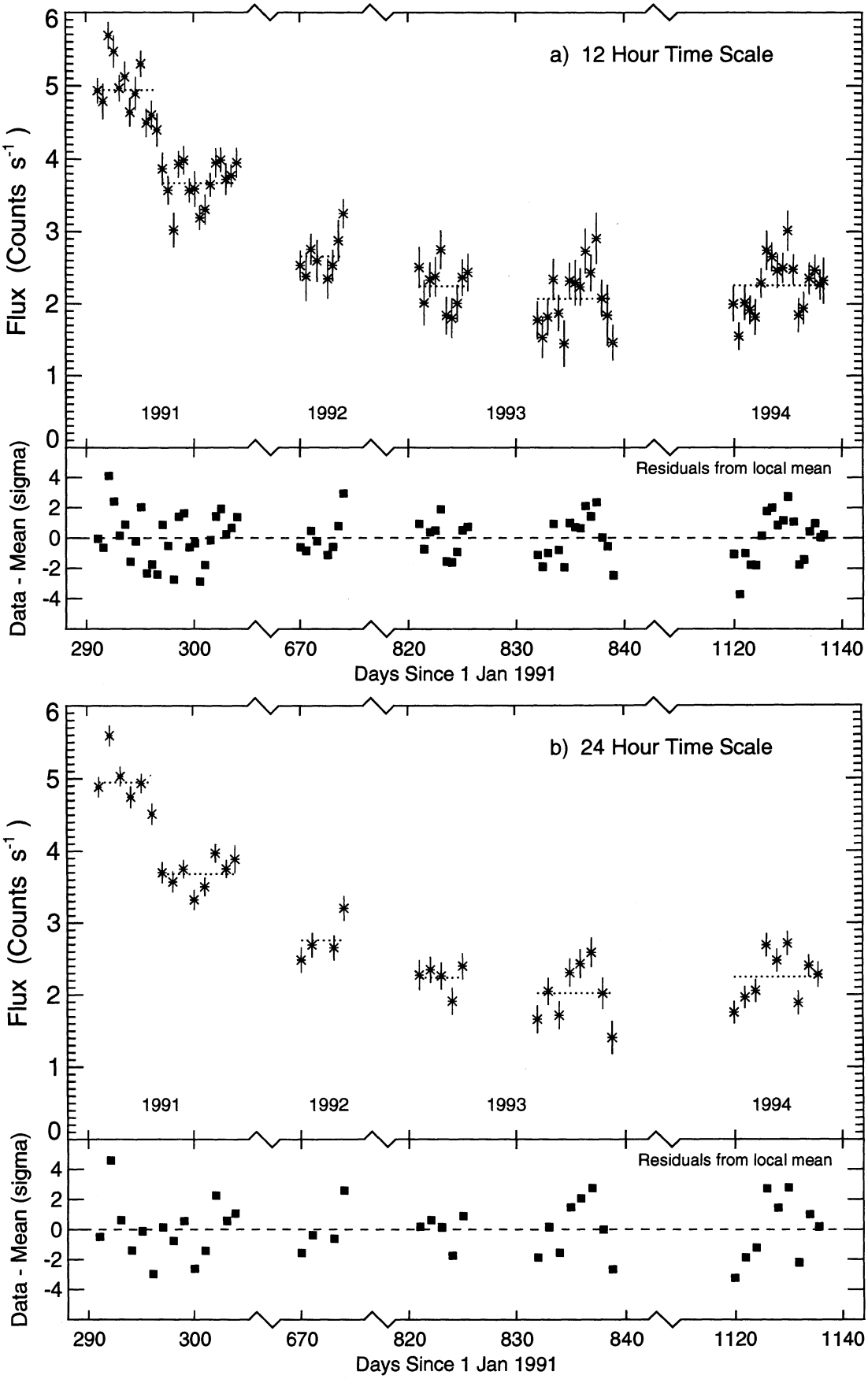

FIG. 1.—Integral intensities in the 40 to 500 keV energy band as a function of time for the 1991, 1992, 1993, and 1994 observations on (*a*) 12 hr and (*b*) 24 hr timescales. Dashed lines in the top panels are long-term averages; points in the lower panels indicate deviations, in units of the relevant standard deviation, from these long-period averages.

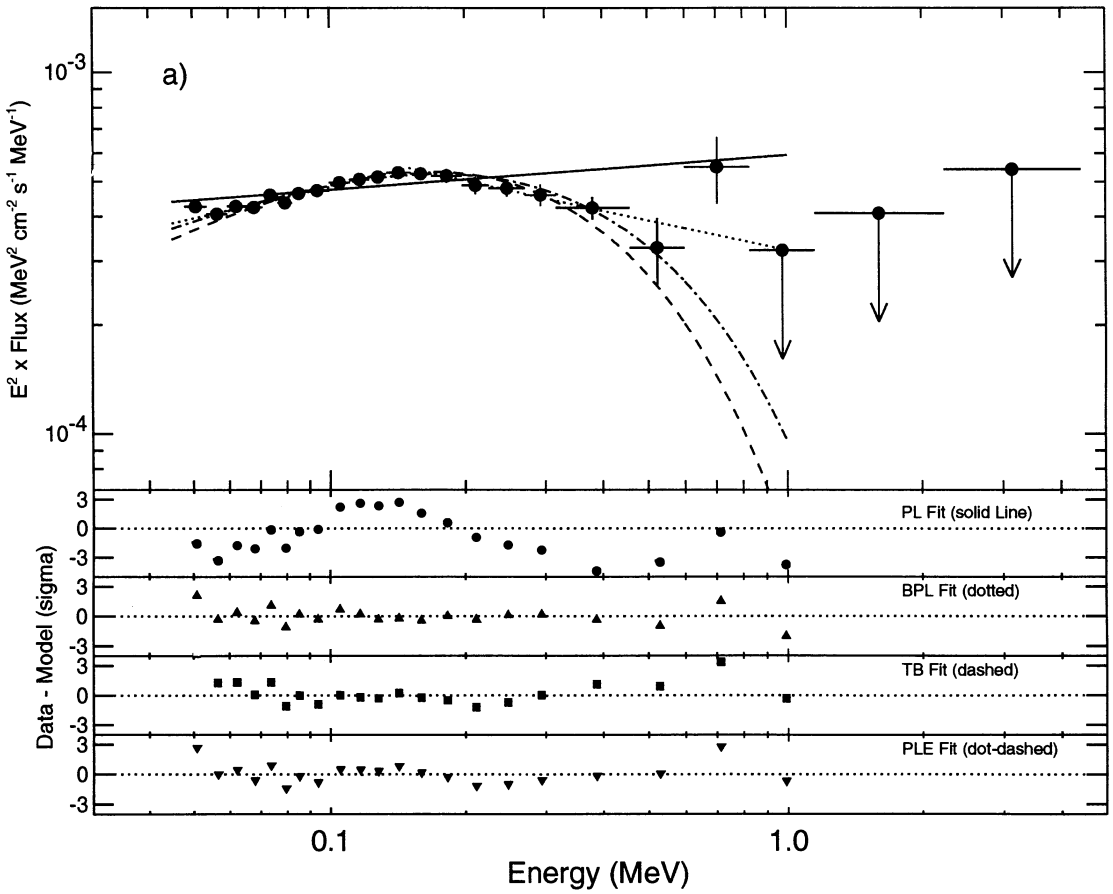

FIG. 2.—Time-integrated differential photon spectra measured in (*a*) the full 1991 observation and (*b*) in the 1992, 1993, and 1994 observations combined. In each figure, least-squares best-fit models shown are a broken power law (*dotted line*), a single power law (*solid line*), a model incorporating a single power law times an exponential (*dot-dashed line*), and a thermal bremsstrahlung spectrum with a Gaunt factor (*dashed line*). Residuals for each fit are shown in the lower panels in units of standard deviations of the data from the best-fit curve.

adequate to characterize the spectral information in the OSSE data; more specific model shapes are not warranted.

The four spectral models were fitted to each spectrum over the 50 to 1000 keV range using a forward-folding technique; results are shown for each spectrum in Figure 2. Table 3 provides fitted parameters and their associated uncertainties. The χ^2 probabilities that the models describe the data sets are also given for each fitted spectrum. The broken power law and the exponentially cutoff power law models provide equally adequate fits to the data for each observation; the precision of the data is not adequate to distinguish between these models. A single power law provides a fully acceptable fit to the combined 1992–1993–1994 low-intensity data, but it does not provide an adequate representation of the higher intensity 1991 data. For the low-intensity data, a model more complicated than a single power law is not required. The thermal model cuts off more sharply than the data at low and high energies and thus does not well characterize the shape of the full spectrum for either intensity level.

The two intensity levels observed in 1991 provide an additional opportunity to study the intensity dependence of the spectral shape. Parameters for the best fits of the four models to these two separate data sets are also given in Table 3. Examination of the fitting parameters for the three different OSSE intensity levels (the 1991 higher intensity level, the 1991 intermediate intensity level, and the 1992–1993–1994 lower intensity level) shows an increasing spectral softening with increase in intensity. Presence of curvature in the low-intensity spectral shape is not required in the fits. However, when viewed in the context of fits to the three intensity levels, the marginally improved fits using the exponentially cutoff power law or the broken power law relative to a single power law at the lowest intensity level may be significant. Figure 3*b* shows spectra for the three intensity levels along with the associated fits of an exponentially cutoff power law. These fits indicate an evolution to lower cutoff energies with increasing intensity, with values ranging from $\sim$300 keV at the highest observed intensities to $\sim$700 keV at the lowest intensity. Similar results for a broken power law model are shown in Figure 3*a*. Below the break energy ($\sim$120–170 keV) the three intensity levels are fitted by a power law with $\Gamma \sim 1.7$ (see Table 3). An intensity-dependent spectral break appears to evolve, relative to this intensity-independent low-energy index, from $\Delta\Gamma = 0.7 \pm 0.15$ at the highest intensities to $\Delta\Gamma = 0.24 \pm 0.10$ at the lowest intensity. The strong covariance between the break energy and the spectral indices above and below the break causes uncertainty in interpreting these curved spectra with a broken power law model, however.

No evidence for gamma-ray line emission was detected from Cen A in the OSSE observations. This is particularly notable for the 0.511 MeV annihilation line, where a 2 σ upper limit for a narrow line (3 keV FWHM) of 2.6×10^{-5} photons cm^{-2} s^{-1}

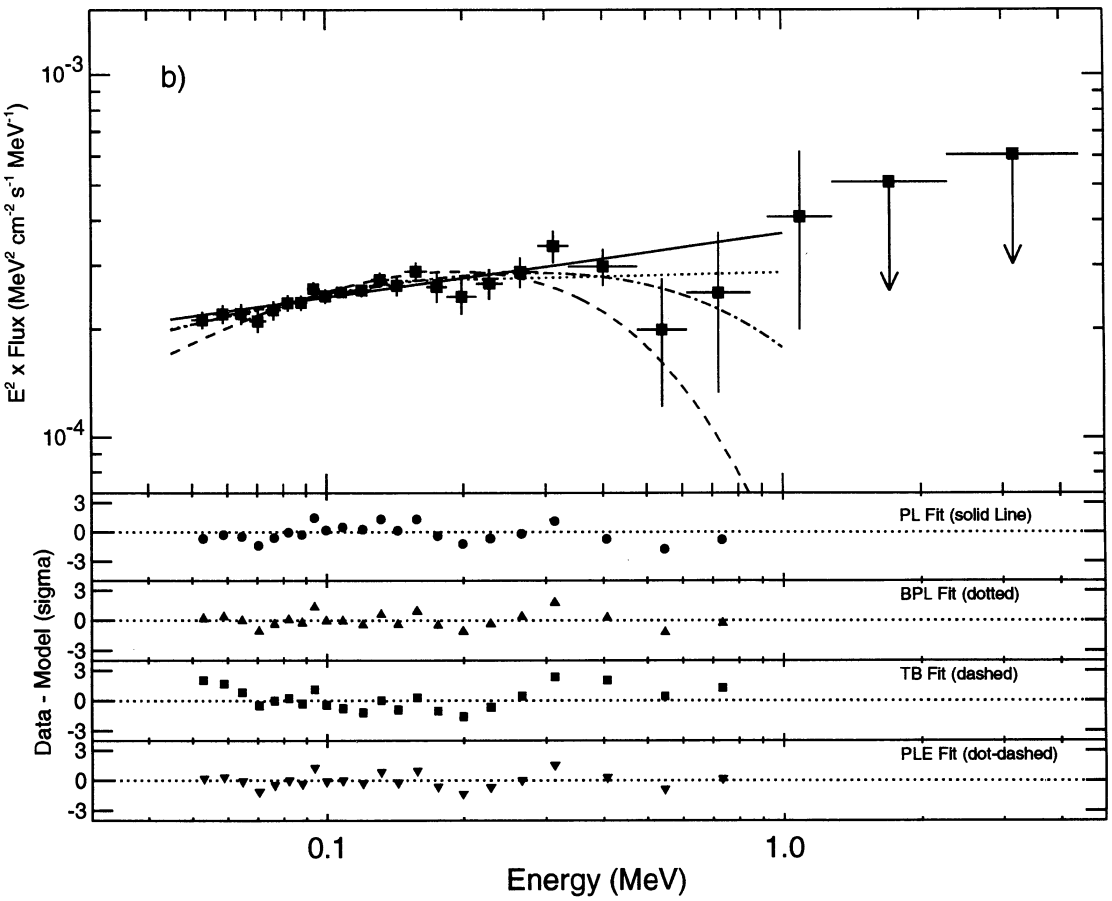

FIG. 2—*Continued*

is established using the full 1991–1994 data set, assuming a broken power-law continuum. This is more than an order of magnitude below previous upper limits set in balloon observations with a NaI spectrometer (Hall et al. 1976), by the *HEAO* A-4 NaI spectrometer (Baity et al. 1981), and by the LEGS germanium balloon-borne spectrometer (Gehrels et al. 1984). Hall et al. (1976) reported detections of broad gamma-ray lines at 1.6 MeV and 4.5 MeV with intensities of $3.4(\pm 1.0) \times 10^{-3}$ and $9.9\ (\pm 3.0) \times 10^{-4}$ photons $cm^{-2}\ s^{-1}$, respectively. At 1.6 MeV, OSSE provides a significantly lower 2 σ upper limit for a broad (400 keV FWHM) line of 9×10^{-5} photons $cm^{-2}\ s^{-1}$. A 2 σ upper limit for a line at 4.43 MeV of 3×10^{-5} photons $cm^{-2}\ s^{-1}$ is also set. If the Hall et al. (1976) observations were valid line detections, then the intensity variability in these lines must be much greater (30–40 times) than that of the continuum at 100 keV (which decreased by a factor of ~ 3 between the two epochs).

4. DISCUSSION

4.1. *Intensity Variations*

OSSE observations have confirmed the long-term variable nature of Cen A at energies below 100 keV (see, e.g., Baity et al. 1981; Jourdain et al. 1993 for summaries), and extended the variability energy range to ~ 500 keV. Our finding that Cen A was at a different average intensity level in each well-separated observation, with mean intensity levels differing by a factor of ~ 2–3 in 28 months, is consistent with the previous observations at hard X-ray energies which have measured intensities differing by about an order of magnitude over two decades. However, the average intensity change within the four isolated intervals observed by OSSE in 1992, 1993, and 1994 was only $\pm 13\%$.

The 12–24 hr timescale for the fastest significant intensity changes which OSSE observed in the 40–500 keV region is significantly shorter than previously reported at hard X-ray energies. Prior to the OSSE observations, the fastest high-energy (100 keV) intensity change observed was by SIGMA in two 1 day observations separated by 4 days (Jourdain et al. 1993). Statistical limitations prevented detection of significant fluctuations within the 1 day SIGMA observations. The OSSE measurements are also statistics-limited at the lowest variability timescales reported. Hints of significant 6 hr variability in the OSSE data suggest that only instrumental sensitivity limitations have precluded measuring shorter term variability; it is likely that we have set only an upper limit to the smallest variability timescale at gamma-ray energies.

The detailed intensity variations in the OSSE observations from five intervals of 4 to 14 days in length over 28 months suggest that Cen A varies on short and long timescales at these energies. Short-term changes appear to have characteristic times as short as 12 to 36 hr; these amplitude changes about persistent levels in each several-day interval are independent of the time-averaged intensity level. The timescale for longer term variability is estimated to be six or more days. The intensity change of $\sim 25\%$ between persistent levels which occurred in

TABLE 3

BEST-FIT MODEL PARAMETER VALUES

Year and Model	Amplitude[a]	E_b or E_0[b]	Γ_1	$\Delta\Gamma$	E_c or kT[b]	χ^2 Probability
1991 (Higher):						
BPL[c]	2.40 ± 0.36	0.166 ± 0.014	1.68 ± 0.03	0.71 ± 0.15	...	0.40
PL[d]	5.51 ± 0.06	0.1	1.88 ± 0.03	...	...	$<10^{-6}$
PL-EXP[e]	5.68 ± 0.05	0.1	1.31 ± 0.07	...	0.254 ± 0.033	0.34
PL-EXP 1.6[f]	5.62 ± 0.05	0.1	1.6	...	0.487 ± 0.036	0.11
TB[g]	5.70 ± 0.05	0.1	...	...	0.219 ± 0.006	0.21
1991 (Lower):						
BPL	2.32 ± 0.48	0.142 ± 0.016	1.74 ± 0.05	0.48 ± 0.10	...	0.86
PL	4.18 ± 0.05	0.1	1.92 ± 0.03	...	...	2.5×10^{-3}
PL-EXP	4.27 ± 0.05	0.1	1.55 ± 0.08	...	0.386 ± 0.086	0.48
PL-EXP 1.6	4.25 ± 0.04	0.1	1.6	...	0.440 ± 0.036	0.52
TB	4.32 ± 0.05	0.1	...	...	0.204 ± 0.007	0.02
1991 (Total):						
BPL	2.42 ± 0.29	0.150 ± 0.009	1.71 ± 0.03	0.57 ± 0.07	...	0.67
PL	4.74 ± 0.04	0.1	1.90 ± 0.02	...	...	$< 10^{-6}$
PL-EXP	4.87 ± 0.04	0.1	1.43 ± 0.05	...	0.305 ± 0.035	0.17
PL-EXP 1.6	4.84 ± 0.04	0.1	1.6	...	0.464 ± 0.025	0.17
TB	4.91 ± 0.03	0.1	...	...	0.211 ± 0.004	0.02
1992 + 1993 + 1994:						
BPL	1.38 ± 0.60	0.140 ± 0.034	1.73 ± 0.05	0.24 ± 0.10	...	0.95
PL	2.44 ± 0.03	0.1	1.82 ± 0.03	...	...	0.75
PL-EXP	2.48 ± 0.03	0.1	1.63 ± 0.07	...	0.765 ± 0.285	0.95
PL-EXP 1.6	2.48 ± 0.03	0.1	1.6	...	0.662 ± 0.077	0.95
TB	2.52 ± 0.03	0.1	...	...	0.243 ± 0.010	0.19

[a] In units of 10^{-2} cm^{-2} s^{-1} MeV^{-1} at E_b or E_0.
[b] Units are MeV.
[c] Double or broken power law (E = energy in MeV; E_b = break energy): $A(E/E_b)^{-\Gamma_1}$ for $E < E_b$; $A(E/E_b)^{-\Gamma_1+\Delta\Gamma}$ for $E > E_b$.
[d] Single power law model: $A(E/E_0)^{-\Gamma_1}$.
[e] Exponentially cut-off power law model: $A(E/E_0)^{-\Gamma_1}e^{-(E-E_0)/E_c}$.
[f] Exponentially cut-off power law model with fixed $\Gamma_1 = 1.6$.
[g] Thermal bremsstrahlung with Gaunt factor: $A(E/E_0)^{-1}e^{-E/kT}g(E, kT)$, where T is the *temperature* and $g(E, kT)$ is the nonrelativistic Gaunt factor.

24 hr or less in the middle of the 14 day 1991 observation provides the strongest support for this longer term variability timescale. The SIGMA measurements also support a timescale of this order. It is principally this longer timescale which has been measured by previous gamma-ray observations with lower statistical precision and/or shorter observation intervals.

Variability has been better studied at lower X-ray energies (2–20 keV) owing to much greater observational coverage and to better counting statistics at these lower energies. At longer timescales, the intensity of Cen A was continuously monitored in this range at low time resolution between 1969 and 1979 by the *Vela 5B* satellite (Terrell 1986) and intermittently by a number of other experiments from 1969 to the present. The long-term (months to years) variation in the relatively sparse set of intensity measurements around 100 keV obtained since 1969 is well correlated with these lower energy X-ray intensity measurements over the past two decades (see Gehrels et al. 1984; Jourdain et al. 1993 for summaries), indicating a common origin for the long–time-base emission over the 2–100 keV region. OSSE's observations of both short ($\sim$12 hr) and long (28 month) timescale correlated intensity changes at energies above and below 100 keV extend this common variability energy range to 500 keV.

The observational case for short-term variability in Cen A at these lower X-ray energies is less clear. Winkler & White (1975) observed a secular increase of 1.8 ± 0.2 over 6 days (3–10 keV); Lawrence, Pye, & Elvis (1977) gave evidence of a flux increase of 1.8 ± 0.4 in about 2 days (2–6 keV). Conflicting observations have been reported at shorter times. The *Einstein Observatory* IPC (Feigelson et al. 1981) detected variations from the nuclear region of Cen A in the 2–6 keV band of 30% in 20 days and a factor of 7 between observations 6 months apart. However, they found no significant short-term variability, setting an upper limit of 3% to variations on 3 hr timescales. In a careful analysis of *HEAO* A-2 data, Tennant & Mushotzsky (1983) similarly found a 2% upper limit to variability on timescales shorter than $\sim$90 minutes. In contrast, *EXOSAT* (Morini, Anselmo, & Molteni 1989) reported rapid variability of typically 10% in the 3–20 keV band, both in the form of linear trends and periodic variations, on timescales of hundreds to thousands of seconds. The OSSE upper limits of 12 to 24 hr to minimum variability timescales at higher energies are not in conflict with these *Einstein* and *HEAO* lower limits, but when combined they do provide interesting bounds to the size of the emitting region, as discussed in § 4.3.

4.2. *Spectra*

A selected set of historical Cen A X-ray and gamma-ray observations at energies above 10 keV are displayed in Figure 4. Only observations with well-defined measurements of the spectrum above 10 keV are included, and we plot only the >10 keV data. Data points with less than 2 σ significance were generally excluded for clarity, although exceptions to this data-selection criterion were made in the high-energy region where few positive detections exist. The recent *CGRO* measurements by OSSE, COMPTEL (Steinle et al. 1994), and EGRET (Fichtel et al. 1994; Hartman 1994) are included. Upper limits shown for OSSE in the 1–10 MeV range as filled circles are

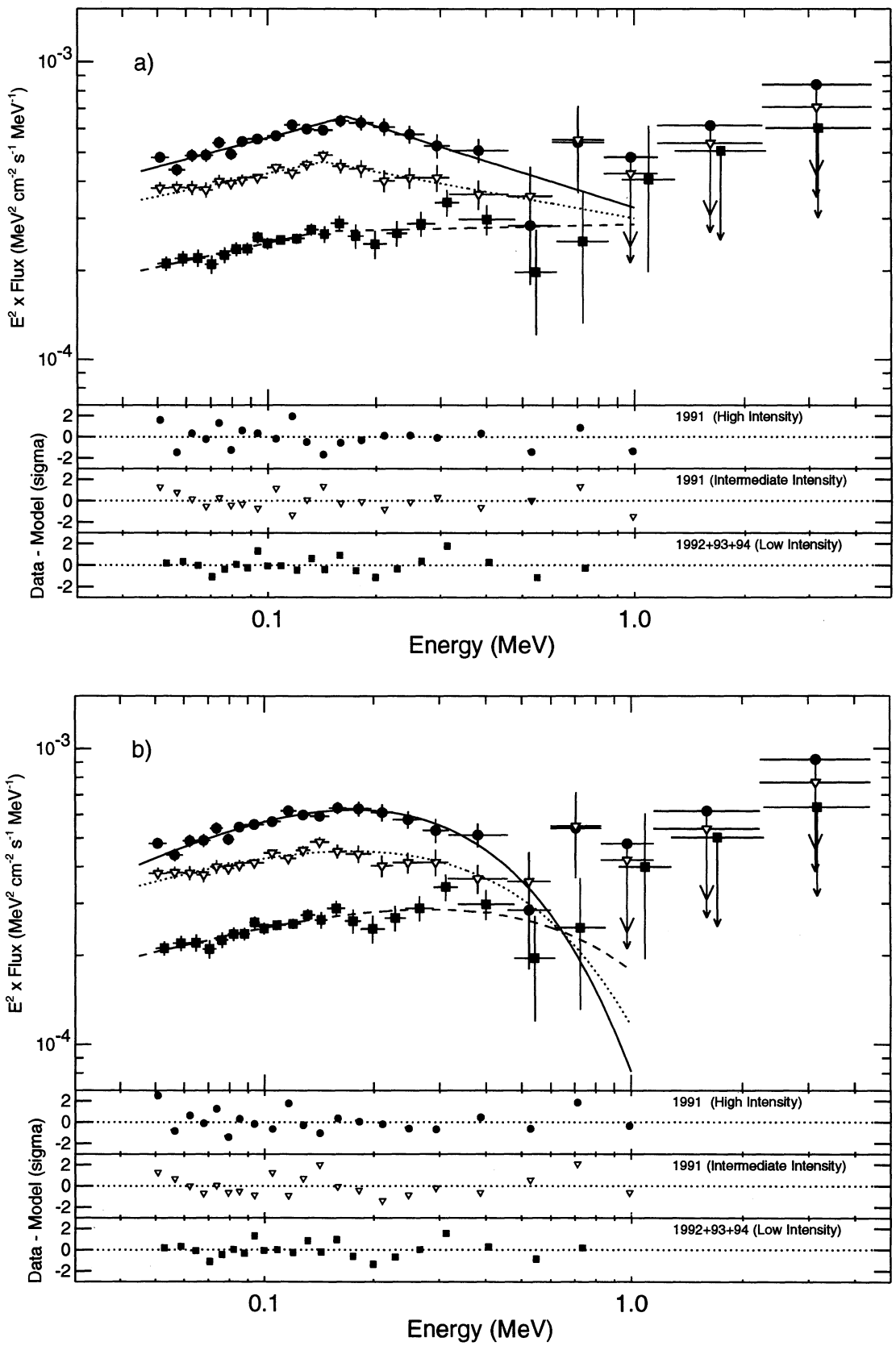

FIG. 3.—Comparisons of OSSE spectra from three intensity levels: the 1991 high intensity level, the 1991 intermediate intensity level, and the 1992–1993–1994 low intensity level. (*a*) Each spectrum is fitted with a broken power-law model. (*b*) Each spectrum is fitted with an exponentially cut-off power-law model. (*c*). Each spectrum is fitted with an exponentially cut-off power-law model, but with the spectral index fixed at 1.6.

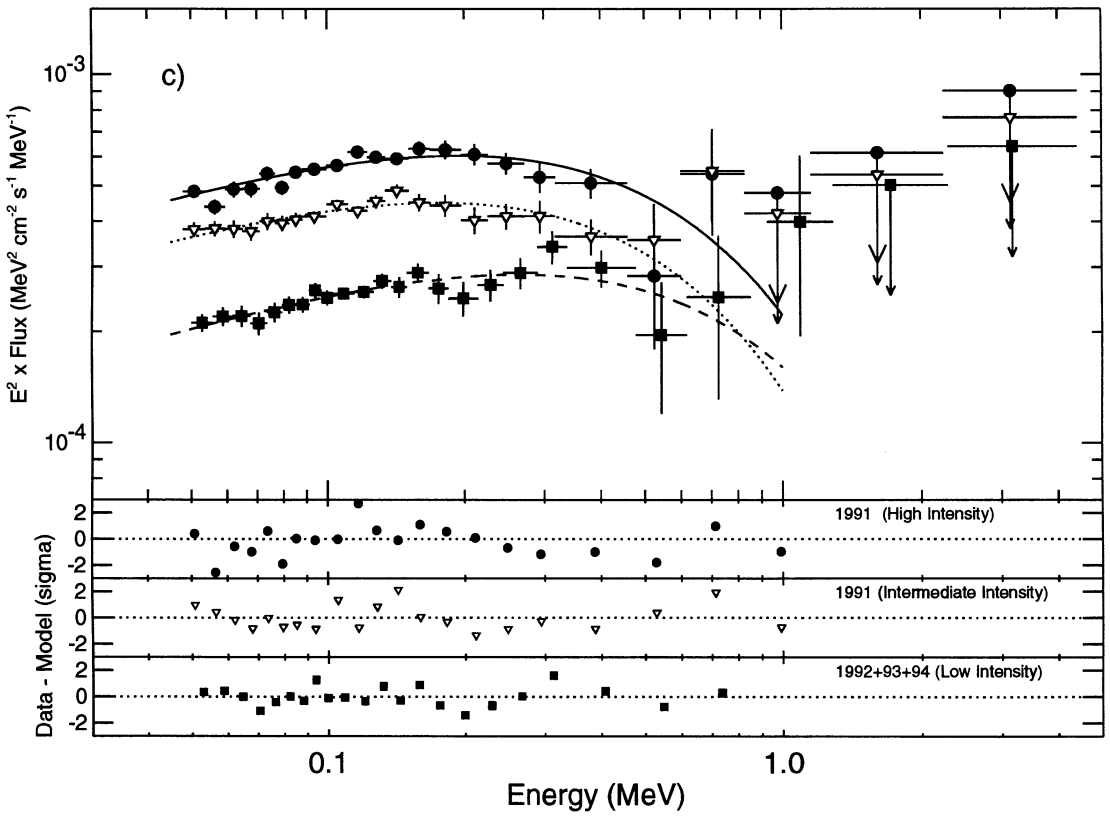

FIG. 3—*Continued*

composite upper limits from the full 1991 observation. The COMPTEL measurements and upper limits are from the summation of a number of observations in two ~1 yr long intervals in 1991–1992 and in 1992–1993. The two EGRET upper limits shown are from observations contemporaneous with the 1991 (VP 12) and the 1994 (VP 316) OSSE observations.

OSSE data support an intensity-dependent evolution in the average spectral shape of Cen A at energies >100 keV. At energies <100 keV, no significant changes in the spectral shape with intensity are found. This is in general agreement with previous reports of >2 keV observations which conclude that the hard X-ray spectral shape of Cen A is intensity independent, with Γ between 1.6 and 1.7 after effects of photoelectric absorption associated with a hydrogen column density $\approx 1.0 \times 10^{23}$ cm^{-2} were removed. Note that the spectral fitting of these earlier observations is dominated by the more statistically significant flux of photons below 100 keV. In experiments where Cen A was observed at least twice with the same instrument at considerably different intensity levels (e.g., Mushotzsky et al. 1978; Baity et al. 1981; Feigelson et al. 1981; Morini et al. 1989; Maisack et al. 1992), Cen A also showed intensity-independent spectral shapes below 100 keV with $1.6 < \Gamma < 1.7$. For example, Jourdain et al. (1993) calculated a weighted mean value of $\Gamma = 1.64$ for the spectral indices of the ensemble of previous higher energy measurements, and Morini et al. (1989) similarly obtained a mean of $\Gamma = 1.69$ for <20 keV measurements. If the OSSE 50–120 keV data are fitted separately, agreement is found with these results, and an intensity-independent power law with $\Gamma = 1.7 \pm 0.08$ represents the three measurements well (see Table 4). Thus, the intensity-dependent spectral evolution detected by OSSE occurs principally above 120 keV.

Spectral shape changes detected by OSSE can be characterized as either increasing spectral curvature with increasing intensity, which is well represented by an exponentially cut-off power law (Fig. 3*b*) with cutoff energies ranging from ~700 keV at the lowest intensities to ~300 keV at the highest intensities, or as a broken power-law spectrum (Fig. 3*a*) with $\Delta\Gamma$ ranging from 0.24 to 0.7 between the lowest and highest intensities. Because these models give statistically equivalent fits to the OSSE data, measurements at higher and lower energies are required to determine which of the two quite different spectral shapes best represents the Cen A spectrum. Because previous measurements down to 2 keV indicate a power-law spectral shape below ~100 keV with spectral index between 1.6 and 1.7, it is reasonable to fix the power-law index in the exponentially cut-off power law in an attempt to obtain a more physical fit to the OSSE data at low energies. Figure 3*c* shows such a fit

TABLE 4

LOW-ENERGY BAND (0.05–0.12 MeV) POWER-LAW[a] FIT PARAMETERS

Year	Amplitude (10^{-2} cm^{-2} s^{-1} MeV^{-1})	Γ	χ^2 Probability
1991 (Higher).....	5.65 ± 0.07	1.62 ± 0.05	0.20
1991 (Lower)	4.23 ± 0.04	1.76 ± 0.04	0.76
1992	2.94 ± 0.08	1.73 ± 0.10	0.15
1993	2.22 ± 0.05	1.72 ± 0.09	0.93
1994	2.42 ± 0.09	1.68 ± 0.14	0.06

[a] Single power-law model: $A(E/E_0)^{-\Gamma}$, with $E_0 = 0.1$ MeV.

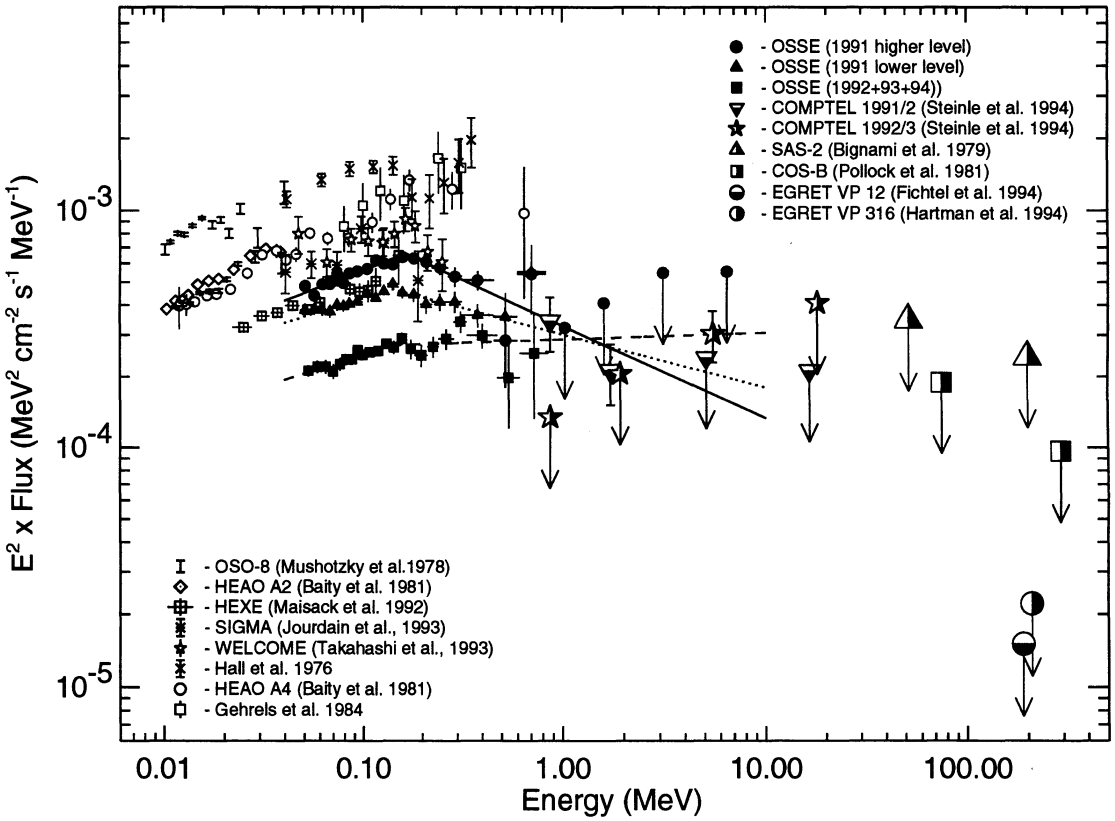

FIG. 4.—Summary plot of selected historical X-ray and gamma-ray spectral measurements for Cen A together with spectra from the three relatively distinct intensity levels observed by OSSE. Measurements included have accurate spectral measurements above 10 keV; data points below 10 keV have been omitted. For clarity, less than 2 σ data points and upper limits have been left off except in the MeV region where few positive detections exist. In this $E^2 \times dN/dE$ plot, a power law with $\Gamma = 2$ would appear as a horizontal line. Best-fit broken power-law spectra for the three OSSE observations are shown by a solid line (1991 higher intensity level), a dotted line (1991 intermediate intensity level), and a dashed line (1992–1993–1994 lower intensity level).

with a fixed index $\Gamma = 1.6$. For $\Gamma = 1.7$ we obtain a significantly less satisfactory fit. Fitting parameters are given in Table 3. The model with $\Gamma = 1.6$ gives a satisfactory fit to the data and suggests that the underlying power law has an index closer to 1.6 than 1.7. Constraining the power-law index increases the cutoff energy at the higher intensities and produces a less satisfactory fit to the data above 120 keV.

The measurement of Hall et al. (1976), *HEAO* A-4 (Baity et al. 1981), Gehrels et al. (1984), and Takahashi et al. (1993) at intensities higher than those observed by OSSE (Fig. 4) lend some support to the broken power-law interpretation of the spectral behavior above 100 keV. Each of these shows power-law behavior below 150 keV which is consistent with $\Gamma = 1.7$ and does not conflict with a break or rollover in the 120–170 keV region, in accord with the OSSE data assuming a broken power-law model. In fact, Baity et al. (1981) reported marginal evidence for a spectral break at 140 keV, and Takahashi et al. (1993) found evidence for a spectral break at 185 keV.

The COMPTEL instrument on *CGRO* provides observations of Cen A which overlap the upper part of the OSSE energy range and extend to 30 MeV. This large field-of-view instrument has made a number of observations of Cen A since 1991. It did not detect Cen A from those data taken contemporaneously with OSSE (Table 1). However, they did detect the source in a summation of several observations in two 1 yr epochs during 1991–1992 and 1992–1993 (Steinle et al. 1995). These data (Fig. 4) cannot be used directly in comparison with a given OSSE observation because of source variability. As can be seen in Figure 4, COMPTEL found strikingly different results in the two sets of measurements. Their findings of both positive fluxes and nondetections in the same energy band in the two epochs, but with $\sim 4\ \sigma$ detections in at least one band in each epoch, suggest spectral shape changes which may be similar to the intensity-dependent shapes observed by OSSE if the broken power-law interpretation is correct. More detailed sensitivity comparisons of the two instruments will be required to fully understand this.

As discussed in § 2, the X-ray–selected BL Lac object 1E 1312−4122 (Stocke et al. 1990), which is located $\sim 2°$ from Cen A, was marginally detected above 100 MeV by EGRET (Fichtel et al. 1994); in recent reanalyses of the EGRET data, this source decreased in significance and could not be differentiated from a source at the position of Cen A (Hartman 1995). Any emission from this source contributes a varying fraction of its intensity to OSSE's measured Cen A spectra, depending on the collimator viewing arrangement as discussed in § 2. COMPTEL cannot discriminate between Cen A and 1E 1312−4122, so that its emission would contribute fully to their measured Cen A spectrum. If this source has a soft gamma-ray spectrum with a larger spectral break in the MeV region, as would be required by the X-ray observations if it has a soft gamma-ray spectrum, it could be contaminating both the OSSE and COMPTEL Cen A spectra at high energies (probably above 1 MeV). By carefully arranging the OSSE source and background field position angles and locations, it would be possible to isolate the contribution of Cen A from

that of 1E 1312−4122 in a future observation. A deep simultaneous OSSE, COMPTEL, and EGRET observation of Cen A to be performed in the near future is designed to achieve this result and to better understand the high-energy behavior of Cen A.

Even though the COMPTEL measurements are not contemporaneous with the OSSE observations, the low flux levels observed by OSSE in each observation in 1992–1994 suggest that the source remained in a relatively low state during this time, so that the 1992–1993 COMPTEL points are probably from intensity levels similar to the lowest OSSE level. The positive COMPTEL observations support models with significant emission at energies above 1 MeV, such as the broken power law. The exponentially cut-off power-law model is in marginal agreement with the 1991–1992 COMPTEL measurement but in disagreement with the single positive 1992–1993 $\sim 4\ \sigma$ data point at ~ 5 MeV.

As discussed above, recent reanalyses of EGRET data found an $\sim 5\ \sigma$ excess in the vicinity of Cen A. EGRET measurements are currently being treated as upper limits to Cen A emission (Hartman 1995). Two sigma upper limits of 1.5×10^{-7} and 2.2×10^{-7} photons cm^{-2} s^{-1} above 100 MeV were obtained from the observations contemporaneous with those by OSSE in 1991 (VP 12, Fichtel et al. 1994) and 1994 (VP 316, Hartman 1994), respectively. These upper limits, as well as those of *SAS 2* and *COS B*, are shown in Figure 4 as differential fluxes assuming an $E^{-3.0}$ power-law spectrum. These limits do not constrain the exponentially cut-off power-law model. However, if EGRET's detected flux is actually from Cen A, this model could be ruled out. The EGRET data points, whether upper limits or actual observations, do provide strong constraints on the OSSE broken power-law spectra. Extrapolation of the OSSE broken power-law model fits, shown by lines in Figure 4, exceed these EGRET upper limits, implying the need for an additional spectral steepening somewhere between a few MeV and 100 MeV.

Cen A has long been thought to have its peak in νF_ν (where ν is the frequency and F_ν is the differential energy flux) in the MeV region (see Gehrels & Cheung 1992 for a recent review). The data in Figure 4 provide new evidence that this peak occurs at soft gamma-ray energies. The OSSE measurements at low to moderate intensity levels show that the spectra have an intensity-dependent break or rollover in the 100–400 keV region relative to the "canonical" low-energy $\Gamma = 1.6$–1.7 power law. During the higher intensity 1991 OSSE observations, the peak energy emission occurs at a spectral "break" or rollover in the 100–300 keV region. At the low-intensity level observed in 1992, 1993, and 1994 the spectrum is considerably harder, and the peak emission moves to higher energies. The OSSE data alone cannot determine the peak emission energy in this case. Assuming a distance to Cen A of 5 Mpc, the luminosities measured with OSSE between 50 and 1000 keV using the broken power-law fits are 7.2, 5.6, and 3.8×10^{42} ergs s^{-1} for the three spectra represented in Figure 4.

It is useful to compare the intensity-dependent spectral behavior of Cen A with that of Cygnus X-1, a well-studied black hole candidate in our Galaxy. Extensive OSSE observations of Cyg X-1 over a 3 yr period show intensity-dependent spectral behavior (Phlips et al. 1995). Although some curvature remains in the Cyg X-1 spectrum at the lowest observed intensities, its spectrum can be approximated by a single power law in the low-intensity state, in close analogy to the low-intensity spectral fit of the Cen A spectrum. As the intensity increases, the Cyg X-1 spectral curvature increases, and the spectra can be represented by an exponentially cut-off power law with a reflection component (e.g., Zdziarski et al. 1994). The intensity-correlated spectral softening above 150 keV is qualitatively similar in the two sources, suggesting similar high-energy processes in these candidate black-hole sources which differ in luminosity by a factor of $\sim 10^5$. However, the intensity-correlated increase in spectral curvature of Cyg X-1 below 100 keV differs from the low-energy spectral behavior of Cen A, where the spectrum remains an intensity-independent power law below ≈ 120 keV.

4.3. *Emission Models*

Valid models for the high-energy radiation from Cen A must be in accord with the following observational results from OSSE and previous experiments: (1) the high-energy radiation varies on timescales $\lesssim 1$ day, implying a size scale of the emitting regions $\lesssim 10^{15}$ cm from light travel–time arguments for a stationary source; (2) the hard X-ray/soft gamma-ray spectra between 2 and ~ 120 keV are characterized by an intensity-independent power-law shape with photon spectral index $\Gamma \sim 1.7$; and (3) a spectral softening occurs at photon energies between ~ 120 keV and 700 keV, with the cutoff energy moving to lower energies with increasing source intensity. When modeling the spectra by a broken power law, the difference $\Delta\Gamma$ between the spectral indices of the lower and upper broken power-law spectrum increases with intensity, indicating increased spectral curvature in the higher intensity states.

The most widely accepted model for persistent luminous emission of AGNs is accretion onto massive black holes. The 50–1000 keV luminosity inferred from the OSSE measurements of Cen A in its high-intensity state is 7×10^{42} ergs s^{-1}, assuming an isotropically radiating source and a distance of 5 Mpc. The measured 50–1000 keV luminosities in the lower intensity states are only a factor ~ 2 lower than in the high-intensity state because of the observed spectral hardening at higher energies. Even in the lowest observed intensity level, the 1992/1993 COMPTEL observations shown in Figure 4 suggest that the peak of the νF_ν spectrum occurs at < 1 MeV. Multivavelength observations (e.g., Gehrels & Cheung 1992) indicate that the soft gamma-ray emission dominates the bolometric luminosity at all wavelength ranges except, possibly, for two regimes. These are the highly obscured UV/soft X-ray energy range, where no information is available, and at lower energies near 10^{12} Hz, where there is evidence (Hawarden et al. 1993) for submillimeter emission from a compact source with luminosity comparable to that measured with OSSE. Within some bolometric correction factor ~ 2, therefore, we find that the total luminosity from the nuclear region of Cen A is $\approx 10^{43}$ ergs s^{-1}.

A luminosity of 10^{43} ergs s^{-1} implies a black hole mass $M \approx 8 \times 10^4\ M_\odot$, assuming Eddington-limited accretion in the Thomson limit. Because photons in the OSSE energy range have energies approaching 511 keV, Klein-Nishina corrections must be applied (Pozdnyakov, Sobol, & Sunyaev 1983; Dermer & Gehrels 1995), which amount to a reduction in the radiation force by a factor 0.86, 0.62, and 0.40 at photon energies of 50, 200, and 511 keV, respectively. Thus, the minimum black hole mass to supply the observed luminosity, if assumed to be isotropic and produced by Eddington-limited accretion, is lowered by a factor of $\approx 30\%$–50% from the Thomson limit estimate. The minimum black hole mass for Cen A from OSSE

observations is therefore $\approx 5 \times 10^4 M_\odot$. If the emission is produced within ≈ 10 Schwarzschild radii of the black hole, then the implied minimum timescale of variability is just $\Delta t \approx 3 \times 10^6 (M/M_\odot)/c \approx 5$ s, which is much shorter than any of the measured variability timescales discussed in § 4.1. It is nevertheless important to identify the shortest variability timescale, since this determines the compactness $l = L\sigma_T/m_e c^3 R$, where $R \approx c\,\Delta t$ is the size scale of the emission region. For Cen A, we find that $l \approx 0.1/\Delta t$(days) from the OSSE measurements. If the *EXOSAT* measurements of rapid variability (Morini et al. 1989) are confirmed, the compactness of Cen A could be as large 10–100.

Even a value of $l \approx 0.1$ can be used to exclude optically thin thermal bremsstrahlung models, since the bremsstrahlung compactness $l_{ff} \approx 0.03\tau_p^2 \theta^{1/2}$ (Skibo et al. 1995), where θ is the effective color temperature of the radiation in units of $m_e c^2$. Even with $\theta = 1$, we require the optical depth $\tau_p \gg 1$ to jointly satisfy the luminosity and time variability constraints, so that Compton scattering would also be important. The observed spectrum of Cen A does not, of course, look like an optically thin thermal bremsstrahlung spectrum unless one considers an appropriate superposition of emitting regions with a range of temperatures.

Because of the low measured value of l, it is not possible to exclude stationary source models in favor of beaming models on the basis of the Elliot & Shapiro (1974) relation or the efficiency limits of Fabian (1979; see Dermer & Gehrels 1995 for a discussion of these constraints). The spectral softening of Cen A at several hundred keV is suggestive of models where thermal electrons with temperature $kT \approx 100$ keV Comptonize a soft photon source. The Sunyaev & Titarchuk (1980) spectral form is only accurate in the low-temperature ($kT/m_e c^2 \ll 1$) diffusion limit ($\tau_p \gg 1$) regime, and cannot be applied directly to the OSSE data from Cen A. The OSSE results are consistent with thermal Comptonization models after high temperature and low optical depth corrections are applied (e.g., Hua & Titarchuk 1995; Skibo et al. 1995). Indeed, models which can be approximated as a power law times an exponential give reasonable fits to the OSSE data over the full OSSE energy range in any intensity state (see Figs. 3*b* and 3*c* and Tables 3 and 4). However, the COMPTEL detection at higher energies (Steinle et al. 1995) makes an exponential function or the sharply truncated thermal Comptonization spectral shape improbable for Cen A, unless a higher temperature component or a pion-production component (Jourdain & Roques 1994) is included.

Models with a strong reflection component (e.g., Lightman & White 1988; Guilbert & Rees 1988) produce a 20–100 keV bump in the hard X-ray region which is not observed in Cen A and can be excluded. The standard nonthermal pair cascade models (e.g., Lightman & Zdziarski 1987; Done & Fabian 1989) can also be excluded by the OSSE data for two reasons. If $l \approx 0.1$, then the cascade is weak, and the spectrum continues without break to high energy, contrary to the high-energy COMPTEL and OSSE data. If, on the other hand $l \gg 1$, as suggested by the *EXOSAT* observations, then we should observe a pronounced pair annihilation line, which has not been observed in the OSSE Cen A spectrum. Of course, a composite thermal/nonthermal model, as proposed by Zdziarski, Lightman, & Maciolek-Niedzwiecki (1993a) for NGC 4151, cannot be ruled out on the basis of spectral considerations. Nonthermal Compton models comprising a source of soft photons and a population of nonthermal electrons which scatter the soft photons to the gamma-ray regime (e.g., Band & Malkan 1989) can also reproduce the observed spectra if the electron spectrum is appropriately tailored.

Beaming models can also be considered for Cen A. However, models where the axis of a jet of relativistically outflowing material is oriented at small angles with respect to our observing direction are not supported by the classification of Cen A as an FR I radio galaxy. High-resolution studies of the nucleus of Cen A show a self-absorbed core and a one-sided steep-spectrum jet component which displays subluminal outflows with transverse velocity $\cong 0.26c$ (Meier et al. 1989, 1993). Although the one-sidedness of the jet is somewhat surprising, its radio properties are in accord with the interpretation that Cen A is a misaligned blazar (Bailey et al. 1986), where the radio jet is beamed away from the observer. Skibo et al. (1994) therefore argue that the high-energy radiation is jet emission scattered into our line of sight and deduce an angle that the jet makes to our line of sight of $61° \pm 5°$, which provides a good fit to the 1991 OSSE data. If the Cen A emission is direct jet radiation, then the incomplete Compton cooling models of Dermer & Schlickeiser (1993) and Sikora, Begelman, & Rees (1994) predict that $\Delta\Gamma \leq 0.5$. This prediction is consistent with the observations except for the highest observed intensity level where $\Delta\Gamma = 0.71 \pm 0.15$, in which case there is a conflict at the 1.5 σ level.

4.4. *Centaurus A, Gamma-Ray Active Galactic Nuclei, and the Diffuse Gamma-Ray Background*

Cen A is probably the best example of a radio-loud AGN viewed at large angles with respect to the jet axis. It has a spectrum unique among AGNs observed at high energies, with emission detected with OSSE at soft gamma-ray energies and with COMPTEL at energies >1 MeV but with no clear detection above 30 MeV by EGRET. Typical radio-quiet Seyfert AGNs display spectra that exponentially soften with an average *e*-folding energy of ~45 keV (Johnson et al. 1994). Radio-loud AGNs detected with OSSE, such as 3C 120 and 3C 390.3, have not been reported as COMPTEL sources although, because of their weaker flux, it is doubtful that they could be detected with COMPTEL even if they had a spectrum like Cen A. Gamma-ray AGNs observed with EGRET at photon energies >30 MeV all have power-law spectra with $1.5 < \Gamma < 2.6$ which extend into the GeV range (Fichtel et al. 1994). These sources are nearly all associated with blazars, which include BL Lac objects and flat-spectrum radio-loud quasars. The combined noncontemporaneous EGRET, COMPTEL, and OSSE observations of bright gamma-ray blazars are consistent with most gamma-ray blazars having a significant spectral steepening in the 1–30 MeV range ($\Delta\Gamma = 0.3$–1.5 for five well-observed sources; see McNaron-Brown et al. 1995). The highly variable emission of Cen A, with a similar spectral break, although at lower energies, suggests that it is observationally intermediate between gamma-ray Seyferts and blazars.

The spectra from the FR I galaxy Cen A, with a misaligned jet, and from the blazar 3C 273 with a nearly aligned jet (see Johnson et al. 1995) show interesting similarities. Both have intensity-independent power-law spectra with $\Gamma \sim 1.7$ at hard X-ray energies, and both display a spectral break or rollover in the soft gamma-ray regime. During at least some observations, both have shown an effective break by as much as $\Delta\Gamma \sim 0.7$. The principal difference between the two sources is in the energy and magnitude of this break. For Cen A, the break

occurs above ~ 120 keV, and a variable value of $\Delta\Gamma$ is measured. For 3C 273, the break is at ~ 1 MeV and $\Delta\Gamma \sim 0.7$ in the one instance when contemporaneous broadband gamma-ray observations were made (Lichti et al. 1994; Johnson et al. 1995). Thus, the two AGNs may be fundamentally similar, with the differences possibly arising from the different jet-viewing angle, as suggested by spectral calculations of jet emission models of Dermer & Schlickeiser (1993) and Baring (1994). These models predict a spectral break at lower energies with larger viewing angles. The similarities of these two AGNs add support to the hypothesis that Cen A is a misaligned blazar.

Lower sensitivity hard X-ray and gamma-ray observations over the past 20 yr have produced snapshot observations of the spectrum of Cen A, clarifying the importance of this type of source to the origin of the extragalactic X-ray and gamma-ray background (EGB). Studies using recent data from OSSE, *Ginga*, and *ROSAT* show that emission from Seyfert galaxies can explain the EGB spectrum up to ~ 100 keV (e.g., Zdziarski et al. 1993b, 1995; Madau, Ghisellini, & Fabian 1993). Padovani et al. (1993) and Stecker, Salamon, & Malkan (1993) suggest that blazars can account for part or all of the EGB above a few MeV. If the spectrum of Cen A is typical of FR I radio galaxies, then this class may contribute significantly to the EGB spectrum in the region between ≈ 50 keV and 1 MeV, although there is currently no evidence in the OSSE data from Cen A for a feature that could explain the origin of the "MeV bump" in the EGB (see, e.g., Kinzer, Johnson & Kurfess 1978; Gruber et al. 1985), where neither Seyferts nor blazars appear to provide significant contributions.

5. CONCLUSIONS

Cen A has been observed with OSSE to emit hard X-ray and low-energy gamma radiation that is variable on both short (12 hr) and long (>4 day) timescales. These observations imply that the radiation is produced by a compact source with characteristic dimensions $\lesssim 10^{15}$ cm. Flux variations at energies less than and greater than 100 keV are correlated on both timescales. No evidence for gamma-ray line emission is detected during the OSSE observations, and 2 σ upper limits for narrow or broad line emission of $< 9 \times 10^{-5}$ photons cm^{-2} s^{-1} above 500 keV are established. The spectral shape at $E < 120$ keV is found to be independent of intensity within the measurement precision, consistent with many previous hard X-ray measurements between ~ 2 and 100 keV of a spectrum with photon number index $\Gamma \cong 1.6$–1.7. The spectral shape above 120 keV displays intensity-correlated evolution and hardens with decreasing intensity. Although these properties significantly constrain emission models, neither isotropic nor jet emission models can be excluded on the basis of the OSSE observations.

The current observations provide new insights into the nature of the active nucleus in Cen A. Many questions are raised by the present study which, however, can only be answered by simultaneous multiwavelength observations. In particular, it is important to determine the bolometric corrections for the different intensity levels observed with OSSE. Contemporaneous OSSE and high-resolution radio observations could establish whether the emergence of subluminal components is correlated with intensity variations. This would address whether the high-energy radiation from Cen A is associated with misaligned jet radiation. Further joint searches with OSSE, COMPTEL, and EGRET on *CGRO* for intensity enhancements of Cen A in the MeV range could be crucial to understanding the origin of the gamma-ray background. Clearly, more observations of Cen A at a variety of intensity levels, correlated with measurements at different wavelengths, will be necessary in order to fully understand this interesting object.

We thank Neil Gehrels, William Paciesas, and Volker Schönfelder for permission to include the VP 316 observations from a multiwavelength observation of Cen A. This work was supported under NASA grant DPR S-10987C.

REFERENCES

Bailey, W., Sparks, J., Hough, D., & Axon, D. 1986, Nature, 322, 150
Baity, W. A., et al. 1981, ApJ, 244, 429
Band, D. L., & Malkan, M. A. 1989, ApJ, 345, 122
Baring, M. G. 1994, in The 2nd Compton Symp., ed. C. Fichtel, N. Gehrels, & J. Norris (New York: AIP), 639
Bassani, L., & Dean, A. 1983, Space Sci. Rev., 35, 367
Bignami, G. F., Fichtel, C. E., Hartman, R. C., & Thompson, D. J. 1979, ApJ, 232, 649
Burns, J., Feigelson, E., & Schreier, E. 1983, ApJ, 273, 128
Dermer, C. D., & Gehrels, N. 1995, ApJ, 447, 103
Dermer, C. D., & Schlickeiser, R. 1993, ApJ, 416, 458
Done, C., & Fabian, A. C. 1989, MNRAS, 240, 81
Ebneter, K., & Balick, B. 1983, PASP, 95, 675
Elliot, J. L., & Shapiro, S. L. 1974, ApJ, 192, L3
Fabian, A. C. 1979, Proc. R. Soc. Lond. A., 366, 449
Feigelson, E. D., Schreier, E. J., Delvaille, J. P., Giacconi, R., Grindlay, J. E., & Lightman, A. P. 1981, ApJ, 251, 31
Fichtel, C. E., et al. 1994, ApJS, 94, 551
Gehrels, N., & Cheung, C. 1992, in Testing The AGN Paradigm, ed. S. Holt, S. Neff, & M. Urry (New York: AIP), 348
Gehrels, N., Cline, T. L., Teegarden, B. J., Paciesas, W. S., Tueller, J., Durouchoux, P., & Hameury, J. 1984, ApJ, 278, 112
Giles, A. B. 1986, MNRAS, 218, 615
Grindlay, J. E., Helmken, H. F., Hanbury Brown, R., Davis, J., & Allen, L. 1975, ApJ, 197, L9
Gruber, D. E., Matteson, J. L., Jung, G. V., & Kinzer, R. L. 1985, in Proc. 19th Internat. Cosmic Ray Conf., ed. F. Jones, J. Adams, & G. Mason (Washington: NASA), 349
Guilbert, P., & Rees, M. J. 1988, MNRAS, 233, 475
Hall, R. D., Meegan, C. A., Walraven, G. D., Djuth, F. T., & Haymes, R. C. 1976, ApJ, 210, 631
Hartman, R. C. 1992, private communication
Hartman, R. C. 1994, private communication
———. 1995, private communication
Hawarden, T. G., Sandell, G., Matthews, H. E., Friberg, P., Watt, G. D., & Smith, P. A. 1993, MNRAS, 260, 844
Hua, X. M., & Titarchuk, L. 1995, ApJ, 449, 188
Johnson, W. N., et al. 1993, ApJS, 86, 693
Johnson, W. N., et al. 1994, in The 2nd Compton Symposium, ed. C. Fichtel, N. Gehrels, & J. Norris (New York: AIP), 515
———. 1995, ApJ, 445, 182
Jourdain, E., et al. 1993, ApJ, 412, 586
Jourdain, E., & Roques, J. P. 1994, ApJ, 426, L11
Joy, M., Harvey, P., Tollestrup, E., Sellgren, K., McGregor, P., & Hyland, A. 1991, ApJ, 366, 82
Kinzer, R. L., Johnson, W. N., & Kurfess, J. D. 1978, ApJ, 222, 370
Kinzer, R. L., et al. 1994, in The 2nd Compton Symp., ed. C. Fichtel, N. Gehrels, & J. Norris (New York: AIP), 531
Lawrence, A., Pye, J., & Elvis, M. 1977, MNRAS, 181, 93P
Lichti, G., et al. 1994, in The 2nd Compton Symp., ed. C. Fichtel, N. Gehrels, & J. Norris (New York: AIP), 611
Lightman, A., & White, T. 1988, ApJ, 335, 57
Lightman, A., & Zdziarski, A. 1987, ApJ, 319, 643
Madau, P., Ghisellini, G., & Fabian, A. 1993, ApJ, 410, L7
Maisack, M., et al. 1992, A&A, 262, 433
McNaron-Brown, K., et al. 1995, ApJ, in press
Meier, D. L., et al. 1989, AJ, 98, 27
———. 1993, in Sub-Arcsecond Radio Astronomy, ed. R. J. Davis & R. S. Booth (Cambridge: Cambridge Univ. Press), 201
Morganti, R., Fosbury, R., Hook, R., Robinson, A., & Tsvetanov, Z. 1992, MNRAS, 256, 1P
Morganti, R., Robinson, A., Fosbury, R. A. E., di Serego Alighieri, S., Tadhunter, C. N., & Malin, D. F. 1991, MNRAS, 249, 91
Morini, M., Anselmo, F., & Molteni, D. 1989, ApJ, 347, 750

Mushotzky, R., Serlemitsos, P., Becker, R., Boldt, E., & Holt, S. 1978, ApJ, 220, 790
O'Neill, T., Tumer, O. T., Zych, A., & White, R. S. 1989, ApJ, 339, 78
Padovani, P., Ghisellini, G., Fabian, A., & Celotti, A. 1993, MNRAS, 260, L21
Phlips, B., et al. 1995, ApJ, submitted
Pietsch, W., Reppin, C., Trümper, J., Voges, W., Lewin, W., Kendriorra, E., & Staubert, R. 1981, A&A, 94, 234
Pollock, A., Bignami, G., Hermsen, W., Kanbach, G., Lichti, G., Mansou, J., Swanenberg, B., & Wills, R. 1981, A&A, 94, 116
Pozdnyakov, L. A., Sobol, J. M., & Sunyaev, R. A. 1983, in Soviet Scientific Reviews, Astrophysics and Space Sciences, Vol. II, ed. R. A. Sunyaev (New York: Harwood), 189
Preston, R., Wehrle, A., Morabito, D., Jauncey, D., Batty, M., Haynes, R., Wright, A., & Nicolson, G. 1983, ApJ, 266, L93
Sikora, M., Begelman, M. C., & Rees, M. J. 1994, ApJ, 421, 153
Skibo, J. G., Dermer, C. D., & Kinzer, R. L. 1994, ApJ, 426, L23
Skibo, J. G., Dermer, C. D., Ramaty, R., & McKinley, J. M. 1995, ApJ, 446, 86
Stecker, F. W., Salamon, M., & Malkan, M. 1993, ApJ, 410, L71
Steinle, H., et al. 1995, Proc. of the COSPAR Gamma-Ray Astronomy Symp., in press
Stocke, J., Morris, S., Giola, I., Maccacaro, T., Schild, R., & Wolter, A. 1990, ApJ, 348, 141
Sunyaev, R. A., & Titarchuk, L. G. 1980, A&A, 86, 121
Takahashi, T., et al. 1993, in Compton Gamma-Ray Observatory, ed. M. Friedlander, N. Gehrels, & D. Macomb (New York: AIP), 523
Tennant, A., & Mushotzky, R. 1983, ApJ, 264, 92
Terrell, J. 1986, ApJ, 300, 669
Ubertini, P., Bazzano, A., Cocchi, M., La Padula, C., & Sood, R, 1993, A&AS, 97, 105
von Ballmoos, P., Diehl, R., & Schönfelder, V. 1987, ApJ, 312, 134
Winkler, P., & White, A. 1975, ApJ, 199, L139
Zdziarski, A., Fabian, A., Nandra, K., Celotti, A., Rees, M., Done, C., Coppi, P., & Madejski, G. 1994, MNRAS, 269, L55
Zdziarski, A., Johnson, W. N., Done, C., Smith, D., & McNaron-Brown, K. 1995, ApJ, 438, L63
Zdziarski, A. A., Lightman, A. P., & Maciolek-Niedzwiecki, A. 1993a, ApJ, 414, L93
Zdziarski, A., Zycki, P., & Krolik, J. 1993b, ApJ, 414, L81